Journal of Organometallic Chemistry 695 (2010) 1863–1868

Contents lists available at ScienceDirect

Journal of Organometallic Chemistry

journal homepage: www.elsevier.com/locate/jorganchem

Synthesis of 1-(1-ferrocenylethyl)-pyridinium chloride and its hybrid materials with lindquist-type polyoxometalates

Yujuan Niu [a], Xiaoyu Ren [a], Bin Yin [a], Danjun Wang [a,b], Ganglin Xue [a,*], Huaiming Hu [a], Feng Fu [b], Jiwu Wang [b]

[a] Key Laboratory of Synthetic and Natural Functional Molecule Chemistry (Ministry of Education), Shaanxi Key Laboratory of Physico-Inorganic Chemistry, Department of Chemistry, Northwest University, Xi'an 710069, China
[b] Shaanxi Key Laboratory of Chemical Reaction Engineering, Yanan University, Yan'an, Shaanxi 716000, China

ARTICLE INFO

Article history:
Received 2 February 2010
Received in revised form
22 April 2010
Accepted 30 April 2010
Available online 6 May 2010

Keywords:
Charge-transfer salts
Ferrocene
Polyoxometalates
Reflectance spectra

ABSTRACT

A new ferrocene derivative, 1-(1-ferrocenylethyl)-pyridinium (fep = CpFeCp–CH(CH_3)–Py^+) chloride, and two charge-transfer salts (CTSs) based on the cationic fep donor and Lindqvist-type polyoxometalate acceptors, $[fep]_2[Mo_6O_{19}]$ (**1**) and $[fep]_2[W_6O_{19}]$ (**2**), were synthesized. fepCl was characterized by elemental analysis, IR spectroscopy and ^1H NMR and the two CTSs were characterized by elemental analysis, IR spectroscopy, UV–vis diffuse reflectance spectrum, cyclic voltammetry, fluorescence spectrum and single crystal X-ray diffraction. X-ray crystallographic studies of the brownish red CTSs **1** and **2** reveal that they are isostructural and crystallize in the monoclinic space group $P2_1/n$. In salts **1**–**2**, fep and polyoxoanions are cocrystallized by Coulombic forces, and there also exist the complex C–H···π and π···π stacking interactions between the adjacent fep cations and C–H···O hydrogen bonds between the adjacent fep cations and polyanions. The UV–vis diffuse reflectance spectra indicate the presence of a broad charge-transfer band between 500 and 850 nm for **1**–**2**, and CT character of **1** and **2** is also confirmed by the Mulliken correlation between the CT transition energies and the reduction potentials of the polyoxometalate acceptors.

1. Introduction

Polyoxometalates (POMs) or metal oxide clusters are versatile in many aspects, and in recent years new efforts have been made to explore their applications in catalysis, medicine, and material sciences [1,2], which is based on the ability of POMs to act as electron reservoirs as well as the extreme variability of their molecular properties, including size, shape, charge, charge density, redox potential, acidity, solubility and so on [3,4]. In particular, the potentialities of molecular materials of these metal oxide clusters are exemplified by the POMs in their use as electron-accepting moieties in charge-transfer materials prepared by cocrystallization with electron-rich organic donors, such as tetrathiafulvalene and their derivatives via an initial electron-transfer [5]. The ferrocene and its derivatives are an excellent type of organicmetallic electron donors, and recent years some charge-transfer salts (CTSs) based on ferrocene-type donor and POM acceptor have been synthesized and structurally characterized [6–13]. The first charge-transfer salt containing the cationic ferrocenyl donor $CpFeCpCH_2N^+(CH_3)_3$ and polyoxometalate acceptors of the Lindqvist structural type ($[M_6O_{19}]^{2-}$) (M = Mo, W) was reported by Professor Kochi in 1995 [10], and he revealed the relevant charge-transfer interactions between POM acceptors and organic donors in the $[C_5H_5FeC_5H_4CH_2N(CH_3)_3]_2M_6O_{19}$ (M = Mo, W) by the UV–vis diffuse reflectance spectrum and time-resolved (laser-flash) spectroscopic method. Recently, our group reported the charge-transfer salts based on the cationic ferrocenyl donor $CpFeCpCH_2N^+(CH_3)_3$ and Keggin-type acceptors, $[CpFeCpCH_2N(CH_3)_3]_4[PMo_{12}O_{40}]\cdot CH_3CN$ and $[CpFeCpCH_2N(CH_3)_3]_4[GeMo_{12}O_{40}]$ [8], in which the Keggin polyanion $\{PMo_{12}O_{40}\}$ was reduced to −4 from the original −3, and $[GeMo_{12}O_{40}]^{4-}$ remains its original oxidation state. The charge-transfer salts composed of cationic donors and anion acceptors can be described as outer-sphere (OS) charge-transfer complexes [14] in which the main interaction between the cation and anion are coulomb force, and the charge-transfer transitions are highly related to the contacts interactions between the cation and anion, and also to the structures and composition of cationic donor and polyoxometalate acceptors. In this direction, we have recently utilized cationic ferrocenylmethylpyridinium donor

* Corresponding author. Tel.: +86 29 8830 2604; fax: +86 29 8830 3798.
E-mail address: xglin707@163.com (G. Xue).

0022-328X/$ – see front matter © 2010 Elsevier B.V. All rights reserved.
doi:10.1016/j.jorganchem.2010.04.033

Table 1
Crystallographic parameters and refinement details for $[fep]_2[Mo_6O_{19}]$ (**1**) and $[fep]_2[W_6O_{19}]$ (**2**).

Compounds	1	2
Formula	$C_{34}H_{36}Fe_2Mo_6N_2O_{19}$	$C_{34}H_{36}Fe_2W_6N_2O_{19}$
M, g mol^{-1}	1463.99	1991.45
Space group	$P2_1/n$	$P2_1/n$
a, Å	12.4674(11)	12.516(2)
b, Å	13.6294(12)	13.681(2)
c, Å	14.0077(13)	14.053(2)
A	90	90
B	114.681(1)	114.705(3)
Γ	90	90
V, Å^3	2162.8(3)	2186.1(6)
Z	2	2
d_{calc}, g cm^{-3}	2.248	3.025
μ, mm^{-1}	2.409	16.436
Total reflns	10,541	10,774
Indep reflns	3834	3878
Parameters	287	263
GOF	1.180	0.932
R_1 ($I > 2\sigma(I)$)	0.0252	0.0378
wR_2 ($I > 2\sigma(I)$)	0.0763	0.0948
R_1 (all data)	0.0319	0.0612
wR_2 (all data)	0.0966	0.1151
Difference in peak and hole, e Å^{-3}	0.569, −0.920	1.565, −1.323

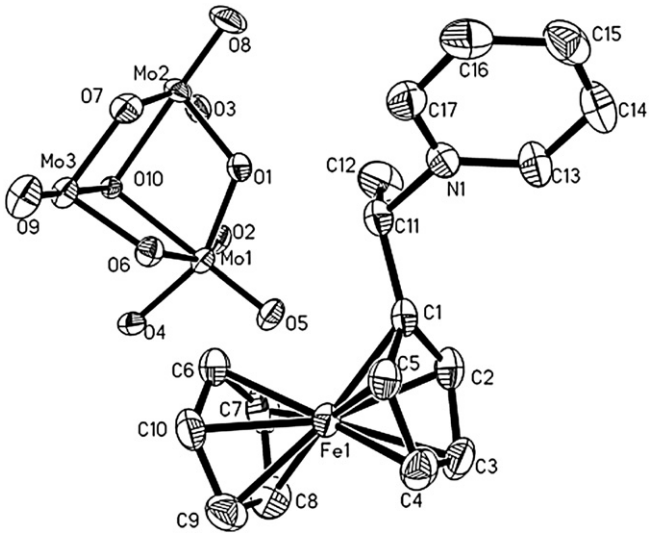

Fig. 1. ORTEP diagram of the asymmetric unit of **1** with the atomic numbering scheme and 30% thermal ellipsoids. H atoms are omitted for clarity.

(CpFeCp–CH_2–Py^+) as cations to obtain four new outer-sphere charge-transfer complexes, $[CpFeCp–CH_2–Py]_2[Mo_6O_{19}]$, $[CpFeCp–CH_2–Py]_2[W_6O_{19}]$, $[CpFeCp–CH_2–Py]_4[W_{10}O_{32}]$ and $(NBu_4)[CpFeCp–CH_2–Py]_2[PMo_{12}O_{40}]$ [13]. In these salts, the ferrocenylmethylpyridinium (CpFeCp–CH_2–Py^+) and the polyoxoanions are cocrystallized by Coulombic forces, and there also exist the complex C–H···π and π···π stacking interactions between the adjacent ferrocenylmethylpyridinium cations. The orbital overlap between the π-donor plane of the pyridyl ring and one oxygen facet of the acceptor octahedron in the solid state is observed in salts $[CpFeCp–CH_2–Py]_2[Mo_6O_{19}]$ and $[CpFeCp–CH_2–Py]_2[W_6O_{19}]$. As a part of our continuing efforts to find new and more suitable cationic donor to tune the crystal stacking structure of charge-transfer complexes based on ferrocenyl cationic donors and polyoxometalate acceptors, herein we report the synthesis of a new cationic ferrocenyl containing pyridinium group, 1-(1-ferrocenylethyl)-pyridinium chloride, and its CTSs with Lindquist-type polyoxometalates.

2. Experimental

2.1. General methods

$(NBu_4)_2M_6O_{19}$ (M = Mo or W) was prepared according to the literature [15]. The solvents used in preparations of fepCl (fep = CpFeCp–$CH(CH_3)$–Py^+) were all dried, especially THF was distilled from Na and pyridine was distilled from NaOH just prior to use, other starting materials were AR grade and used as purchased. ^{1}H NMR spectra were recorded on a Varian INOVA-400 MHz spectrometer with TMS as an internal standard. IR spectra were obtained on an EQUINOX55 IR spectrometer with KBr pellets. Solid state diffuse reflectance spectra between 300 and 850 nm were obtained for the dry pressed disk samples using a Shimazu UV-2550 spectrophotometer, equipped with an integrating sphere coated with polytetrafluoroethylene (PTFE). Absorption spectra were referenced to barium sulfate. Cyclic voltammetry (CV) studies were carried out in acetonitrile solution at ambient temperature under the protection of N_2 using an EG & G 273A apparatus under computer control (M270 software). The source, mounting, and polishing of the glassy carbon (GC, 3 mm diameter) have been described [16]. SCE (saturated calomel electrode) was as the reference electrode, and a platinum wire as the counter electrode, NBu_4Br was the supporting electrolyte, and the scan rate was 100 mV s^{-1}. Luminescent spectra were measured at room temperature on a Hitachi F4500 fluorescence spectrophotometer. Magnetic measurements were carried out using a Quantum Design MPMS-XL SQUID magnetometer.

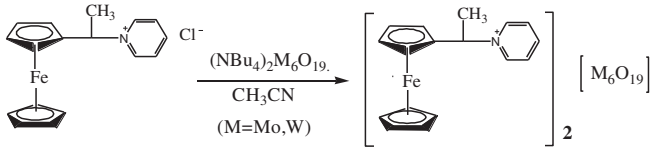

Scheme 1.

2.2. Synthesis of 1-(1-ferrocenylethyl)-pyridinium chloride (fepCl)

A solution of 46.2 g (0.2 mol) of acetylferrocene [17] in 200 ml of ethanol was added dropwise, at room temperature, to a solution of

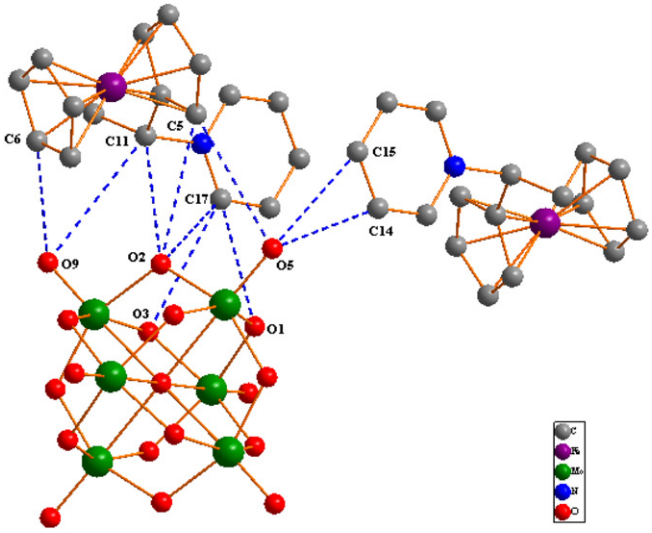

Fig. 2. A representation showing the linkages of hydrogen bonding between the polyoxoanions and the ferrocenyl cations in **1**, H atoms are omitted for clarity.

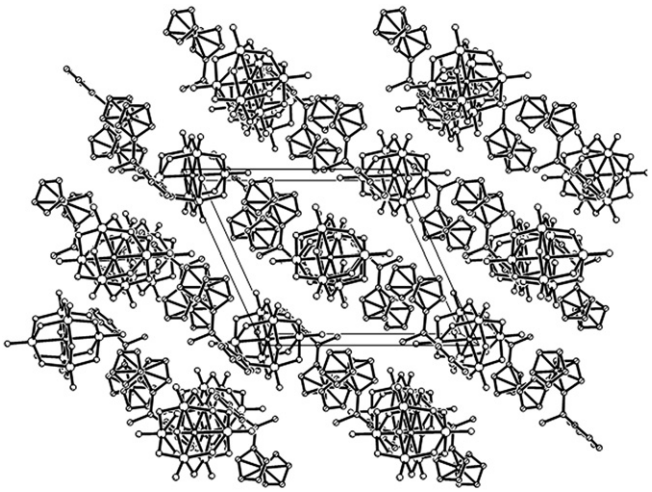

Fig. 3. Projection of the crystal structure of **1** along *b* direction showing the layers of the organic donor and inorganic acceptor alternatively arranged in (10ī) plane and pyridyl rings penetrate into the anion layers. H atoms are omitted for clarity.

30.4 g (0.8 mol) of sodium borohydride in 200 ml of water. The reaction mixture was stirred overnight at room temperature, then poured into water and vacuum filtration, washed and dried, the product 1-hydroxyethylferrocene were obtained [18].

A solution of PCl_3 (0.1 ml, 1 mmol) in THF (5 ml) was added dropwise to a THF (20 ml) solution of (1-hydroxyethyl)ferrocene (0.23 g, 1 mmol) and pyridine (0.1 ml, 1 mmol) at 0 °C. The mixture was left stirring for 1 h at this temperature, the ice bath was removed and the mixture left to stir at room temperature for 3 h. The yellow precipitate formed was filtered off and recrystallisation from CH_2Cl_2, yield: 55.2%. Elemental analysis (%) calcd for $C_{17}H_{18}ClFeN$: C 62.3, H 5.54, N 4.27; found: C 62.0, H 5.75, N 4.14; IR (KBr): 3051(s), 1628(s), 1483(s), 1382(m), 1339(m), 1248(m), 1130 (s), 1055(m), 1031(m), 828(s), 755(s), 730(s) and 681(s) cm^{-1}. ^1H NMR [DMSO-d_6, 400 MHz]: δ 9.10(2H, py), 8.55 (1H, py), 8.13 (2H, py), 5.61 (1H, CH), 4.58 (2H, Cp H), 4.32 (2H, Cp H), 4.26 (5H, Cp H), 1.38 (3H, CH_3), 3.36 (H_2O) and 2.51 (DMSO).

2.3. Synthesis of [CpFeCp–CH(CH_3)–Py]$_2$[Mo_6O_{19}] (**1**)

A solution of fepCl (0.33 g, 1 mmol) in acetonitrile (10 ml) was added dropwise to an acetonitrile (20 ml) solution of $(NBu_4)_2Mo_6O_{19}$ (0.68 g, 0.5 mmol). The mixture was left stirring at room temperature and then filtered. The filtrate was slowly evaporated at ambient conditions. Within 2 days, brownish red block crystals of **1** were isolated in about 55% (based on $(NBu_4)_2Mo_6O_{19}$). Elemental analysis (%) calcd for $C_{34}H_{36}O_{19}Fe_2N_2Mo_6$: C 27.9, H 2.49, N 1.91; found: C 27.3, H 1.86, N 2.06; IR (KBr): 3073.6 (m), 1330.7 (m), 1242.4 (m), 1126.9 (s), 955.6 (vs), 903.4 (s), 796.2 (vs), 675.2 (s).

2.4. Synthesis of [CpFeCp–CH(CH_3)–Py]$_2$[W_6O_{19}] (**2**)

The synthetic procedure for **2** is similar to that of **1** except for using $(NBu_4)_2W_6O_{19}$ (0.95 g•, 0.5 mmol) instead of $(NBu_4)_2Mo_6O_{19}$. The brownish red block crystals of 2 were isolated in about 75% (based on $(NBu_4)_2W_6O_{19}$). Elemental analysis (%) calcd for $C_{34}H_{36}O_{19}Fe_2N_2W_6$: C 20.5, H 1.82, N 1.41; found: C 20.1, H 1.74, N 1.38; IR (KBr): 3075.9 (s), 1330.9 (m) 124,205 (m), 1129.2 (s), 974.5.0 (vs), 880.2 (s), 809.9 (vs), 678.7 (s).

2.5. Crystal structure determination

A selected crystal of compounds **1**–**2** was respectively mounted on a glass fiber capillary which was put on a BRUKER SMART APEX II CCD diffractometer equipped with graphite monochromatic radiation and used for data collection. Data were collected at 293 (**2**) K using MoKα radiation (λ = 0.71073 Å). The structure were solved by direct methods (SHELXTL-97) and refined by the full-matrix-block least-squares method on F^2. All non-hydrogen atoms were refined with anisotropic displacement parameters. Hydrogen atoms were included at calculated positions and refined with a riding model. A summary of the crystal data, experimental details, and refinement results for the structure of **1**–**2** are listed in Table 1. The CCDC reference numbers are CCDC 762166 for **1** and 762167 for **2**.

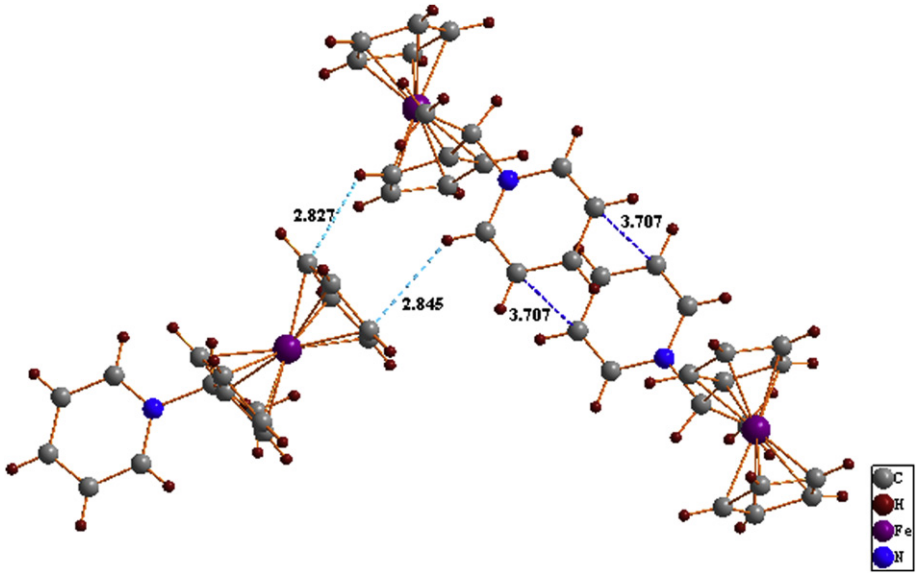

Fig. 4. A view of the interactions between adjacent ferrocenyl units in **1**. The blue short distance between two adjacent pyridyl rings show π···π stacking interactions and the light blue short distance between the hydrogen atom of pyridyl and the bare Cp ring of another adjacent ferrocenyl unit show C–H···π interactions. (For interpretation of the references to color in this figure legend, the reader is referred to the web version of this article.)

Table 2
Characteristic absorptions arising from polyoxoanions (cm^{-1}).

Compound	ν_{as}(M–Oa)	ν_{as}(M–Ob)		ν_{as}(M–Oc)
1	955	903	796	675
$[NBu_4]_2[Mo_6O_{19}]$	957	884	800	662
2	974	880	806	678
$[NBu_4]_2[W_6O_{19}]$	973	877	811	667

3. Results and discussion

3.1. Synthesis and crystal structures

The CTSs **1**–**2** were synthesized by reaction of the corresponding Lindquist anions $[NBu_4]_2[M_6O_{19}]$ (M = Mo, W) with fepCl in CH_3CN solution (Scheme 1). When the yellow dilute acetonitrile solution of fepCl was mixed with the $(Bu_4N)_2[M_6O_{19}]$ (M = Mo, W) acetonitrile solution, the color of reaction mixture changed from yellow to brown. The remarkable color change suggests that the electronic interaction between the cationic ferrocenyl donor and the POM acceptor has occurred [19,20]. Using $(NBu_4)_4Mo_8O_{26}$ instead of $(NBu_4)_2Mo_6O_{19}$ to react in the same conditions, we got the same product **1** in high yield (58%). This is because $[Mo_8O_{26}]^{4-}$ and $[Mo_6O_{19}]^{2-}$ can transform mutually in some conditions [21,22].

Salts **1** and **2** are isostructural and crystallize in the monoclinic space group $P2_1/n$, therefore only the structure of **1** is discussed here. The asymmetric unit of **1** is composed from half of $[Mo_6O_{19}]^{2-}$ and one fep cation and the ratio is 1:2 (Fig. 1). Each anion with the Mo–Oa, Mo–Ob and Mo–Oc average distances of 1.679, 1.924 and 2.316 Å, respectively, is surrounded by twelve adjacent fep units, and there exist several short contacts among the $[Mo_6O_{19}]^{2-}$ polyoxoanions and the fep cations and the nearest C···O distances are in the range of 3.069 (**5**)–3.569(**6**) Å, which shows the presence of interactions between the polyoxoanions and the ferrocenyl via Coulombic forces and CH···O hydrogen bonds (Fig. 2). Fig. 3 shows the packing of the compound in solid state along *b* direction, the layers of polyoxoanions and ferrocenyl cations are alternatively arranged in (10$\bar{1}$) plane, and pyridyl rings penetrate into the anion layers with the closest C···O distance of 3.069(**5**) Å. The ferrocene unit displays the typical sandwich geometry with the two Cp rings in nearly eclipsed conformation. The average dihedral angle between the two Cp rings is only 0.81, in other words the two Cp rings in each ferrocene moiety are almost parallel, which is smaller than 3.5 in $[CpFeCpCH_2N(CH_3)_3]_2[M_6O_{19}]$ (M = Mo,W) [10]. In (10$\bar{1}$) plane the closest Fe···Fe distance between the neighboring ferrocenyl cations is 7.229 Å, adjacent ferrocene units are linked via pairs of C–H···π interactions between the hydrogen atoms of pyridyl and Cp rings of one molecule and the bare Cp ring of the next in the plane, and there also exist π···π stacking interaction between the neighboring pyridyl rings in (101) plane with the mean interplanar separation of 3.583 Å (Fig. 4).

3.2. IR spectra

The absorption peaks in the range 1100–500 cm^{-1} arising from the polyoxoanions for $[NBu_4]_2[Mo_6O_{19}]$, $[NBu_4]_2[W_6O_{19}]$, salts **1** and **2** are compared in Table 2. The ν_{as}(M–Oa) vibration frequencies for **1** and **2** have slightly changes of 1–2 cm^{-1} compared with $[NBu_4]_2[Mo_6O_{19}]$ and $[NBu_4]_2[W_6O_{19}]$, however the frequencies of ν_{as}(M–Ob) and ν_{as}(M–Oc) present larger change, particularly the ν_{as}(M–Oc) for **1** and **2** have blue shifts of 11 and 13 cm^{-1}, respectively. These results indicate that the polyanions in compounds **1** and **2** still maintain the basic Lindquist structure but are distorted owing to the interactions among the ferrocenyl cations and the framework oxygen atoms of polyoxometalates.

3.3. Electronic absorption spectra

UV–vis absorption spectra were obtained by the diffuse reflectance technique [10,23]. The reflectance electronic spectra of the compounds **1**, **2** and starting materials fepCl, $[NBu_4]_2[M_6O_{19}]$ (M = Mo, W) are compared in Fig. 5. It is noticeable that the starting materials did not show any absorption at $\lambda > 500$ nm and the diffuse reflectance spectrum of CTS **1** in the solid state (Fig. 5a) showed a broad strong absorption band from 350 to 800 nm. Spectral (digital) subtraction of the component spectra (i.e. of $[NBu_4]_2[Mo_6O_{19}]$ and fepCl, individually) of salt **1** in the solid state yielded the difference spectrum (Fig. 5a inset) consisting of a very climbing band from 500 to beyond 800 nm, the result is comparable with those of reported charge-transfer salts [10,13]. The diffuse reflectance spectrum of the salt **2** in the solid state (Fig. 5b) is similar to CTS **1**, but it showed a little difference, the climbing band starts from 350 nm and it has downtrend at 750 nm. In accord with Mulliken theory [24–26], the new (visible) absorption bands should be ascribed to charge-transfer transitions between the cationic ferrocenyl donor and the POM acceptors.

3.4. Cyclic voltammetry

Cyclic voltammetry of the CTSs **1**, **2** and the starting materials are showed in Fig. 6. In the range −1.5–1.0 V, CTS **1** exhibits two

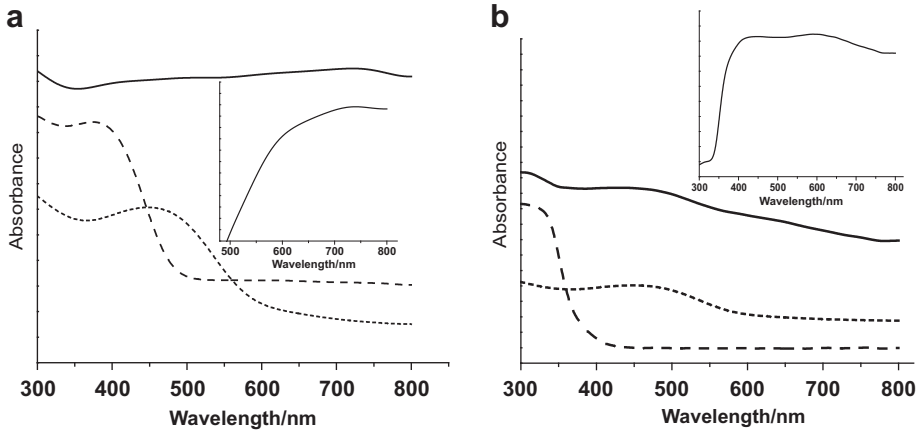

Fig. 5. Charge-transfer absorption spectra of CTs **1** (a) and **2** (b) (——) dispersed in barium sulfate in comparison with the absorption spectra of $[NBu_4]_2[M_6O_{19}]$ (M = Mo, W) (– – –), respectively, and fepCl (·····). The inset elicits the charge-transfer band by the spectral (digital) subtraction of $[NBu_4]_2[M_6O_{19}]$ and fepCl individually from **1** to **2**, respectively.

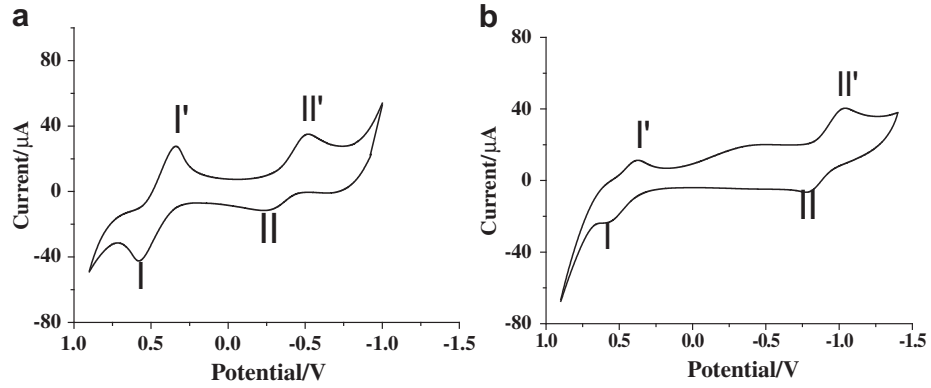

Fig. 6. Cyclic voltammetry of CTSs **1** (a) and **2** (b) in 1×10^{-4} mol/L acetonitrile solution and 0.1 mol/L NBu_4Br as the supporting electrolyte.

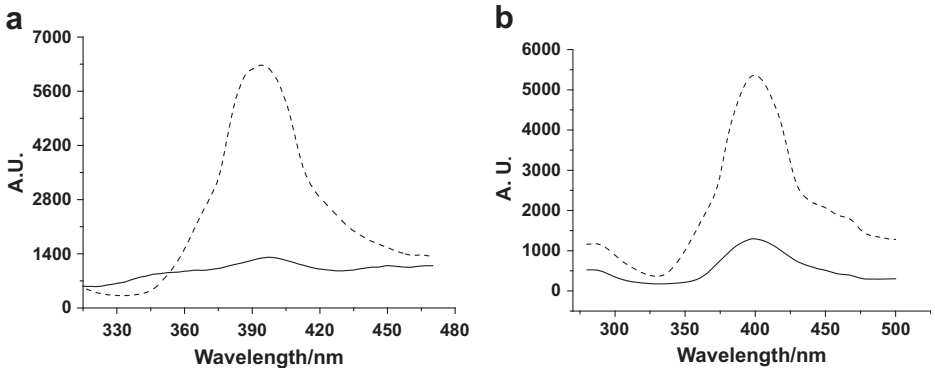

Fig. 7. Emission spectra of the charge-transfer salts **1** (a) and **2** (b) (——), and the corresponding POMs (– – –).

redox pairs (see Fig. 6a), which could be assigned to fep and $Mo_6O_{19}^{2-}$ systems, respectively. E_{mid} value of redox pair for fep in the charge-transfer salt **1** is 0.409 V compared with 0.374 V of free fep cation, and that of the pair for Mo_6O_{19} are −0.365 V compared with −0.445 V of $[NBu_4]_2[Mo_6O_{19}]$. **2** also shows two redox pairs at 0.474 and −0.909 V (see Fig. 6b), which could be assigned to fep and $W_6O_{19}^{2-}$ systems, higher than −0.923 of parent $[W_6O_{19}]^{2-}$ cluster and that of fepCl respectively. The closer value of the reduction wave to that of donor $CpFeCp{-}CH(CH_3){-}Py^+$ for $[Mo_6O_{19}]^{2-}$ than $[W_6O_{19}]^{2-}$ system indicated the more pronounced charge-transfer absorption for **1** than **2**, which is consistent with the spectral extension from 500 nm to the long waves of the hexamolybdate CT salt **1** relative to the hexatungstate analogue **2** in the UV–vis absorption spectra [10].

3.5. Fluorescence properties

The photoluminescent properties of POMs and salts **1**–**2** were investigated in the solid state at room temperature (Fig. 7). Excitation at 280 nm leads to broad fluorescence signals with the emission peaks at about 394, 399 nm for **1** and **2**, respectively, which may mainly be attributed to O2p to Mo4d (or W5d) charge-transfer. The emission bands of 1 and 2 are compared to that of the corresponding POMs and exhibit the weakened fluorescence signals, the obviously distinct suggests the strongly interactions between the ferrocenyl donor to POM acceptors.

4. Conclusion

In summary, a new ferrocene derivative, 1-(1-ferrocenylethyl)-pyridinium chloride, and two charge-transfer salts based on the cationic ferrocenylethylpyridinium donor and Lindqvist-type polyoxometalate acceptors, $[fep]_2[Mo_6O_{19}]$ (**1**) and $[fep]_2[W_6O_{19}]$ (**2**), were synthesized. X-ray crystallographic studies of the crystalline materials reveal that there exist extensive C–H···π and π···π stacking interactions between the adjacent fep cations, and C–H···O hydrogen bonds between the adjacent fep cations and polyanions. The electronic spectra of the **1** and **2** show the charge-transfer absorption band between the cationic ferrocenyl donor and the POM acceptors, and CT character of **1** and **2** is also confirmed by the Mulliken correlation between the CT transition energies and the reduction potentials of the polyoxometalate acceptors. Novel charge-transfer salts could be expected by modulating the ferrocene derivative donors and POMs.

Acknowledgements

This work was supported by the National Natural Science Foundation of China (20973133), the Education Commission of Shaanxi Province (09JK783) and National Training Fund for the Basic Sciences (J083417/J0104).

Appendix. Supplementary material

CCDC 762166 and 762167 contain the supplementary crystallographic data for this paper. These data can be obtained free of charge from The Cambridge Crystallographic Data Centre via www.ccdc.cam.ac.uk/data_request/cif.

Supplementary data associated with this article can be found in the online version, at doi:10.1016/j.jorganchem.2010.04.033.

References

[1] M.T. Pope, Heteropoly and Isopoly Oxometalates. Springer-Verlag, Berlin, 1983.
[2] M. Clemente-León, E. Coronado, C.J. Gómez-García, E. Martinez-Ferrero, J. Clust. Sci. 13 (2002) 381–407.
[3] L. Ouahab, Chem. Mater. 9 (1997) 1909–1926.
[4] E. Coronado, J.R. Galán-Mascarós, C. Giménez-Saiz, C.J. Gómez-García, Adv. Mater. Opt. Electron. 8 (1998) 61–76.
[5] E. Coronado, C.J. Gómez-García, Chem. Rev. 98 (1998) 273–296.
[6] P. Le Maguerès, L. Ouahab, S. Golhen, D. Grandjean, O. Pená, J.C. Jegaden, C. J. Gómez-García, P. Delhaès, Inorg. Chem. 33 (1994) 5180–5187.
[7] S. Golhen, L. Ouahab, D. Grandjean, P. Molinié, Inorg. Chem. 37 (1998) 1499–1506.
[8] Z.F. Li, B. Liu, H.S. Xu, G.L. Xue, H.M. Hu, F. Fu, J.W. Wang, J. Organomet. Chem. 694 (2009) 2210–2216.
[9] W.B. Yang, C.Z. Lu, C.D. Wu, Y.Q. Yu, Q.Z. Zhang, S.M. Chen, J. Clust. Sci. 14 (2003) 421–430.
[10] P.L. Veya, J.K. Kochi, J. Organomet. Chem. 488 (1995) C4–C8.
[11] X.M. Liu, G.L. Xue, H.M. Hu, Q.C. Gao, F. Fu, J.W. Wang, J. Mol. Struct. 787 (2006) 101–105.
[12] Z.F. Li, R.R. Cui, B. Liu, G.L. Xue, H.M. Hu, F. Fu, J.W. Wang, J. Mol. Struct. 920 (2009) 436–440.
[13] H.S. Xu, Z.F. Li, B. Liu, G.L. Xue, H.M. Hu, F. Fu, J.W. Wang, Cryst. Growth Des. 10 (2010) 1096–1103.
[14] S.V. Rosokha, J.K. Kochi, Acc. Chem. Res. 41 (2008) 641–653.
[15] W.G. Klemperer, in: A.P. Ginsberg (Ed.), Inorganic Synthesis, vol. 27, Wiley, New York, 1990, p. 71.
[16] B. Keita, Y.W. Lu, L. Nadjo, R. Contant, M. Abbessi, J. Canny, M. Richet, J. Electroanal. Chem. 477 (1999) 146–157.
[17] P.J. Graham, R.V. Lindsey, G.W. Parshall, M.L. Peterson, G.M. Whitman, J. Am. Chem. Soc. 79 (1957) 3416–3420.
[18] P.J. Swarts, M. Immelman, G.J. Lamprecht, S.E. Greyling, J.C. Swarts, S. Afr. J. Chem. 50 (1997) 208–216.
[19] M. Che, M. Fournier, J.P. Launay, J. Chem. Phys. 71 (1979) 1954–1960.
[20] C. Sanchez, J. Livage, J.P. Launay, M. Fournier, Y. Jeannin, J. Am. Chem. Soc. 104 (1982) 3194–3202.
[21] J. Kang, J.A. Nelson, M. Lu, B.H. Xie, Zh.H. Peng, D.R. Powel, Inorg. Chem. 43 (2004) 6408–6413.
[22] Y. Zhu, L.Sh. Wang, J. Hao, Z.Ch. Xiao, Y.G. Wei, Y. Wang, Cryst. Growth Des. 9 (2009) 3509–3518.
[23] P. Le Maguerès, S.M. Hubig, S.V. Lindeman, P. Veya, J.K. Kochi, J. Am. Chem. Soc. 122 (2000) 10073–10082.
[24] R. Foster, Organic Charge-Transfer Complexes. Academic, New York, 1969.
[25] R.S. Mulliken, J. Am. Chem. Soc. 74 (1952) 811–824.
[26] R.S. Mulliken, W.B. Person, Molecular Complexes. A Lecture and Reprint Volume. Wiley, New York, 1969.